Development of an Emergency Braking System for Teleoperated Vehicles Based on Lidar Sensor Data

Johannes Wallner, Tito Tang and Markus Lienkamp
[1]*Institute of Automotive Technology, Technische Universität München, Boltzmannstr. 15, 85748 Garching b. München, Germany*

Keywords: Emergency Braking System, Teleoperated Vehicles, Lidar Sensor Raw Data, Particle Filter, Motion Prediction.

Abstract: A lidar-based approach of an emergency braking system for teleoperated vehicles is presented. Despite the time delay for the communication link of a teleoperated system, the vehicle has to be able to react to emerging objects in time. Starting with intelligent sensor data processing, reliable information is computed. An adapted particle filter algorithm tracks moving points to calculate their mean velocity, used for the prediction of surrounding moving objects. Further, in order to interpret this information, a situation assessment based on an intervention concept derived from Kamm's circle is implemented. A motion prediction of possible trajectories of the ego-vehicle results in a clear decision-making process. All calculations are made at the raw data level and can be done online. Through artificial objects being included in real sensor data, the methodology was validated.

1 INTRODUCTION

In the case of teleoperated vehicles an operator replaces the real driver. Teleoperated driving is considered to be an intermediate step towards permanently increasing automation of vehicles. Due to the human operator, more complex traffic situations than in fully automated systems can be managed (Diermeyer et al., 2011). One of the challenges is the time delay for the communication link between the operator and the vehicle, which impedes a fast reaction compared to a normal attentive driver. To guarantee a safety level comparable to normal driving, the vehicle must be equipped with an automatic emergency braking system to avoid collisions. Further information on teleoperated road vehicles and the system design for such a vehicle can be found in (Chen et al., 2007) (Ware and Pan, 2011) (Tang et al., 2013) (Gnatzig et al., 2013).

The test vehicle, an AUDI Q7, is equipped with a lidar sensor in the front, as shown in Figure 1. The following approach is characterized by the exclusive usage of the data of this sensor. The reflection points are the only input of the braking system. The output is a decision whether emergency braking is required or not. This approach could also be used in autonomous driving vehicles and has low requirements on the sensor configuration.

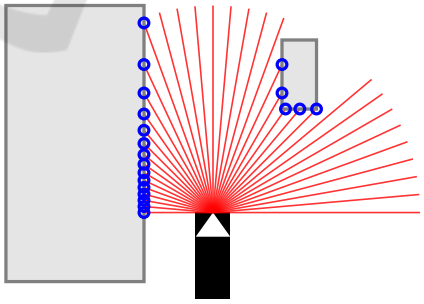

Figure 1: Operating mode of the lidar sensor.

2 STATE OF THE ART

2.1 Categorization on Basis of Specifications

There are already existing automatic emergency braking systems on the market. A categorization into three different types is made on the basis of specifications: Forward collision warning, which detects a potential collision and warns the driver, Collision Mitigation Braking System (CMBS), which detects a potential collision and applies an emergency brake automatically when the collision has become inevitable, and collision avoidance, which can take action to fully avoid a potential collision (Grover et al., 2013, p. 1).

Wallner J., Tang T. and Lienkamp M..
Development of an Emergency Braking System for Teleoperated Vehicles Based on Lidar Sensor Data.
DOI: 10.5220/0005114905690576
In *Proceedings of the 11th International Conference on Informatics in Control, Automation and Robotics* (ICINCO-2014), pages 569-576
ISBN: 978-989-758-040-6

2.2 Intervention Strategies

Based on specifications of an emergency braking system the intervention strategy depends on the braking deceleration, instant of time for braking and initial velocity. The strategy here was presented first by KOPISCHKE and shown amongst others in (Kämpchen, 2007, p. 189), (Jansson et al., 2002), (Hong et al., 2008) and (Stämpfle and Branz, 2008, p. 13). The basis of this strategy is a vehicle with the velocity v_{ego} heading for a static obstacle, illustrated in Figure 2.

A constant deceleration a_{brake} results in a braking distance d_{brake} depending on the ego velocity v_{ego} where a collision can be avoided successfully:

$$d_{brake} = \frac{v_{ego}^2}{2 \cdot a_{brake}}. \quad (1)$$

The minimum distance for an obstacle avoidance maneuver with a constant lateral acceleration a_y is:

$$d_{avoid} = v_{ego} \cdot \sqrt{\frac{w_{ego} + w_{ob}}{a_y}}, \quad (2)$$

where w_{ego} and w_{ob} are the widths of the ego-vehicle and the obstacle.

Calculating the distances d_{brake} and d_{avoid} as a function of the ego velocity v_{ego} leads to the diagram in Figure 3. It is obvious that up to a velocity v_{crit} a collision can be avoided by braking exclusively.

3 SENSOR DATA PROCESSING

The SICK LMS291-S05 lidar sensor of the test vehicle samples the environment with 181 measurement points at a frequency of $f = 75\,\text{Hz}$. To reduce the total amount of points that need to be checked, filtering is essential. Measurement points of static and dynamic objects are filtered separately.

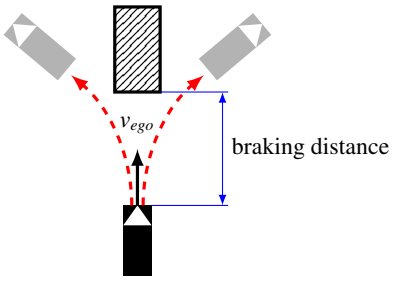

Figure 2: Test scenario with an ego-vehicle heading for a static obstacle.

3.1 Filtering of Static Objects

The filtering for static objects bases on the area that can be reached with vehicle dynamics (Schmidt et al., 2005). Assuming a constant velocity v_{ego} and a constant lateral acceleration a_y, a vehicle moves on a circular path with radius r:

$$r = \frac{v_{ego}^2}{a_y}. \quad (3)$$

The distance of the segment of a circle d_c that is driven over in a period of time Δt is

$$d_c = v_{ego} \cdot \Delta t. \quad (4)$$

For variable lateral accelerations the angle for each segment of a circle calculates as follows:

$$\gamma = \frac{d_c}{r} = \frac{a_y}{v_{ego}} \cdot \Delta t. \quad (5)$$

The endpoints of these trajectories result in an area that can be reached with vehicle dynamics with constant lateral acceleration. This area is shown exemplary for $v_{ego} = 9\,\text{m/s}$ and $\Delta t = 5s$ in Figure 4. Every (static) measurement point outside of this area is filtered out to reduce computational effort.

3.2 Filtering of Dynamic Objects

3.2.1 Detection of Dynamic Points

The detection of dynamic points is achieved by a dynamic threshold operation. Assuming a minimum speed for dynamic objects of v_{min} their measurement points have to be moved during one time step dt for at least

$$d_{min} = v_{min} \cdot dt. \quad (6)$$

Only points moving fast enough are passed on to the next step.

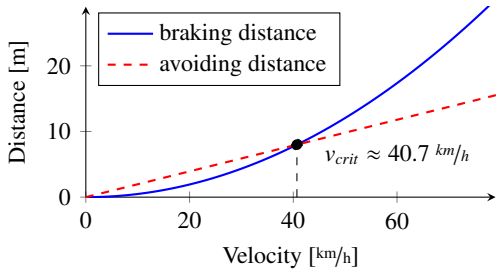

Figure 3: Braking distance and avoiding distance as a function of the initial ego velocity for $a_y = 8\,\text{m/s}^2$, $a_{brake} = 8\,\text{m/s}^2$, $w_{ego} = 2\,\text{m}$ and $w_{ob} = 2\,\text{m}$, see (Stämpfle and Branz, 2008, p. 13) (Jansson et al., 2002).

3.2.2 Grouping and Selection

To reduce the number of moving points even more the points are grouped. The longitudinal and the lateral distance between two points is weighted differently, the threshold depends on the distance like in (Thuy and Puente Leon, 2009) and the maximum size of one group of points is limited.

After the grouping step just two points of each group are selected: therefore the two points of the lateral edge of each group are moved to the minimum longitudinal distance of this group. Thus the movement of the underlying object is represented robustly. The steps of grouping, translation and selection are shown in Figure 5. It is obvious that if the point at the top right is grouped with the right object in a later time step, what is quite plausible, the selected points of the right object won't move that much. It is therefore easier to track them in the following step.

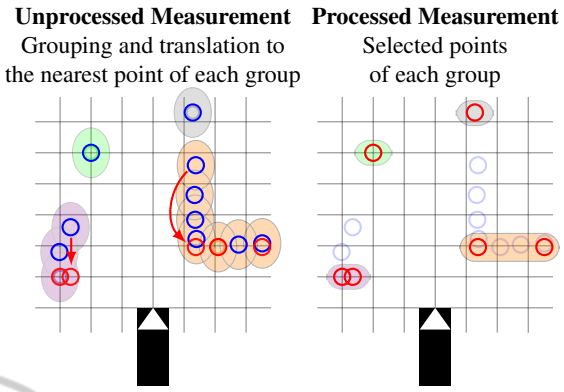

Figure 5: Grouping and selection of points.

3.3 Particle Filter

To track the selected dynamic points from the last subsection an adapted particle filter is used. For a theoretical background of particle filters for tracking applications, see e.g. (Almeida and Araujo, 2008) (Ristic et al., 2004). The approach here is summarized in Figure 6.

Each particle is modeled by an underlying constant velocity movement model. With the steps prediction, computing weights and a resampling step, realized with an algorithm from (Thrun, 2013), it is possible to get reliable information about the amount and direction of the velocity of objects.

After sorting all particles according to their weights, an amount p of the best particles is chosen and a mean velocity for each dynamic object is calculated. The result is a predicted direction of motion of dynamic objects exemplary illustrated for $t_{predict} = 2\,\mathrm{s}$ in Figure 7.

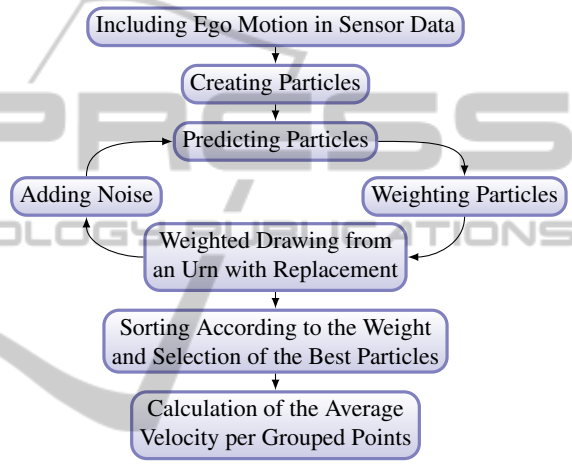

Figure 6: Overview of the particle filter algorithm.

4 SITUATION ASSESSMENT AND BRAKING DECISION

4.1 Intervention Concept

The intervention concept is defined by a range of possible accelerations, which is provided to the operator.

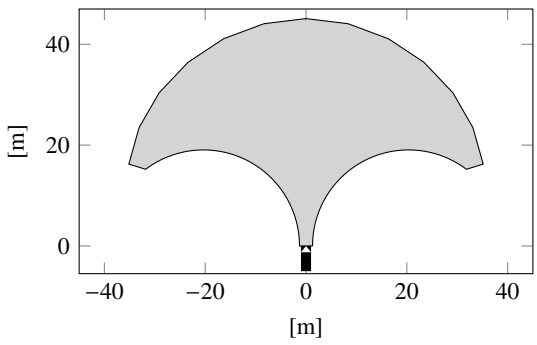

Figure 4: Relevant area for sensor data filtering.

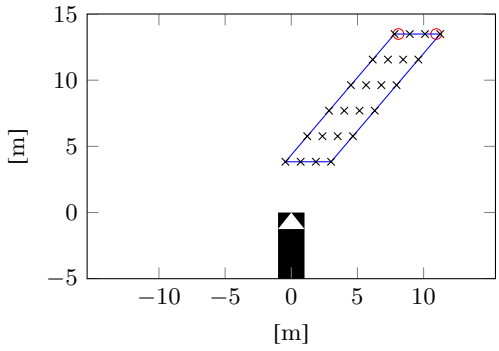

Figure 7: Prediction of a moving object.

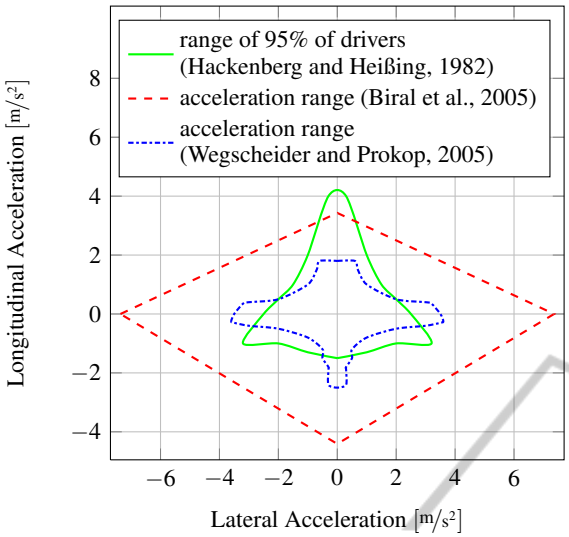

Figure 8: Exemplary acceleration ranges for normal driving situations .

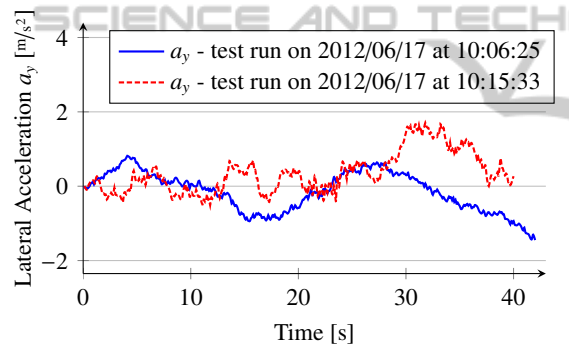

Figure 9: Lateral acceleration in speed range of city traffic during test run.

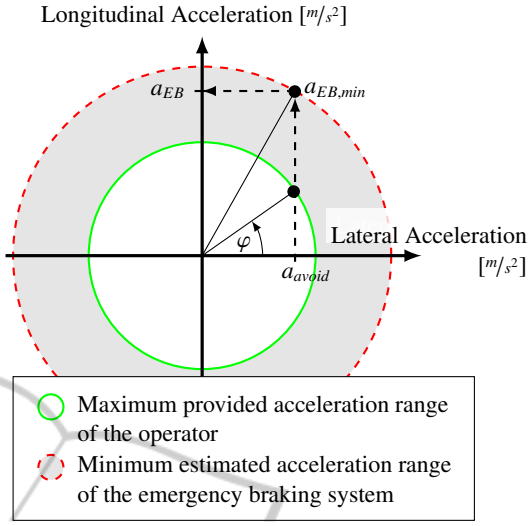

Figure 10: Principle of the intervention concept based on Kamm's circle.

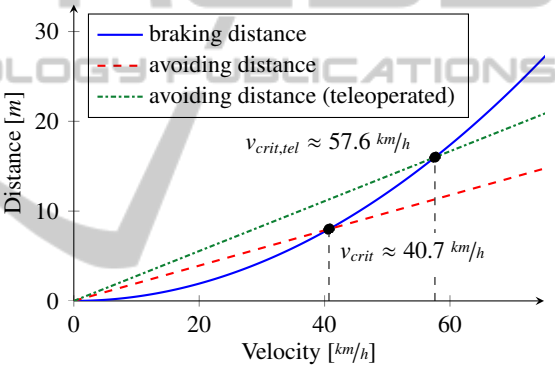

Figure 11: Speed range of full collision avoidance of the emergency braking system.

Usually normal drives take place in specific acceleration ranges. Some exemplary acceleration ranges for normal driving situations of different studies are shown in Figure 8.

A test run with the experimental vehicle in speed ranges of city traffic shows similar results. All accelerations remain within an interval of $[-2,2]$ m/s², as can be seen in Figure 9. These plotted test runs were carried out in normal drive mode, but teleoperated vehicles are limited to a maximum lateral acceleration of $|2\,\text{m/s}^2|$. Therefore, this approach is applicable.

In this specific application of teleoperated vehicles, an acceleration range up to $|a_{max}| = 4\,\text{m/s}^2$ is provided to the operator. This method is based on the principle of Kamm's circle, summarized in Figure 10. If a potential collision cannot be avoided within the green circle from the operator, the emergency braking system intervenes and brakes automatically within the minimal estimated acceleration range in the red circle.

With a supposed emergency braking deceleration $a_{EB,min} = 8\,\text{m/s}^2$ and a lateral avoiding maneuver acceleration $a_y = 4\,\text{m/s}^2$, the intervention of the presented emergency braking system occurs earlier. Therefore the critical velocity of Figure 3 rises up to $v_{crit,tel} \approx 57.6\,\text{km/h}$ where collisions can be avoided successfully, illustrated in Figure 11. The value of $a_{EB,min} = 8\,\text{m/s}^2$ is chosen intentionally low in case of varying friction coefficients.

4.2 Motion Prediction of the Ego-Vehicle by Trajectories

Combining all possible lateral and longitudinal accelerations in Figure 10 by varying φ yields to emergency braking trajectories that offer the opportunity to predict the motion of the ego-vehicle in case of a braking maneuver. The length of these emergency

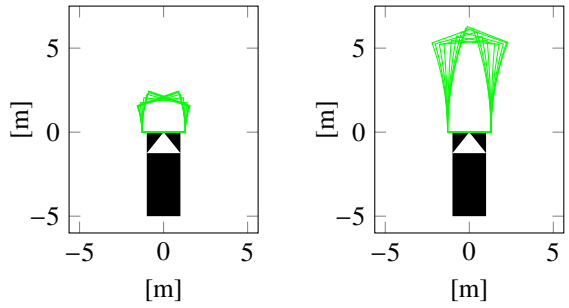

(a) $v_{ego} = 4\,\mathrm{m/s}$ (b) $v_{ego} = 8\,\mathrm{m/s}$

Figure 12: Motion prediction by trajectories.

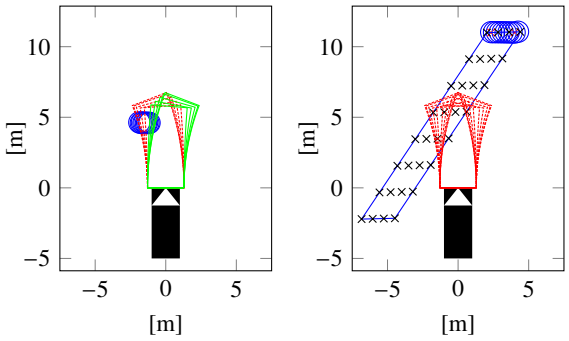

(a) Partially occupied (b) Completely occupied

Figure 13: Decision making process by trajectories.

braking trajectories d_{EB}, respectively the braking distance with constant lateral acceleration, is

$$d_{EB} = \frac{v_{ego}^2}{2 \cdot a_{EB}}. \tag{7}$$

The trajectories for an emergency braking deceleration $a_{EB,min} = 8\,\mathrm{m/s^2}$ and a maximum lateral acceleration of $a_{y,max} = 4\,\mathrm{m/s^2}$ are shown exemplary for two different velocities in Figure 12.

For teleoperated vehicles there is a possibility to limit the number of trajectories to the one already chosen by the operator. The big benefit of a motion prediction of the ego-vehicle by trajectories is that the whole decision making process as to whether emergency braking is required is simplified and these trajectories just have to be checked for trafficability.

4.3 Decision-Making Process.

The decision-making process distinguishes between drivable and occupied trajectories. If all trajectories are occupied over a certain time period, emergency braking is triggered. In Figure 13(a) some trajectories are occupied, but because of the existing possibility to avoid the obstacle, no emergency braking is required. The situation in Figure 13(b) is different, where no avoiding or braking maneuver in the acceleration range of the operator can avoid the collision. Therefore in this case the emergency system would trigger a braking action.

5 VALIDATION WITH REAL SENSOR DATA

5.1 Generation of Artificial Objects in Real Sensor Data

To validate the presented system, artificial objects were generated and included in real sensor data. In this way it was possible to generate various different situations without losing the challenge of real sensor data. The two created test runs, one for a static and one for a dynamic object, are shown in Figure 14. Because of errors in the data of the lidar sensor (measurement points appear randomly at wrong positions), it is advantageous not to brake until n time steps with all trajectories being occupied to reduce faulty activations. In this case a value of $n = 5$ for a time increment of $dt = 0.01\,\mathrm{s}$ has proved to be useful.

5.2 Analysis of the Test Runs

The system triggers the emergency braking in all test cases early enough and avoids collisions successfully. One exemplary setting with a dynamic object is shown in Figure 15. In Figure 15(a) an approaching and correctly predicted object is shown. At $t = 14.07\,\mathrm{s}$ in Figure 15(b) some trajectories are occupied for the first time. In Figure 15(c) all trajectories are occupied, but because of new drivable trajectories in Figure 15(d) less than 0.05 s after the non drivable event emergency braking is not triggered until $t = 14.29\,\mathrm{s}$

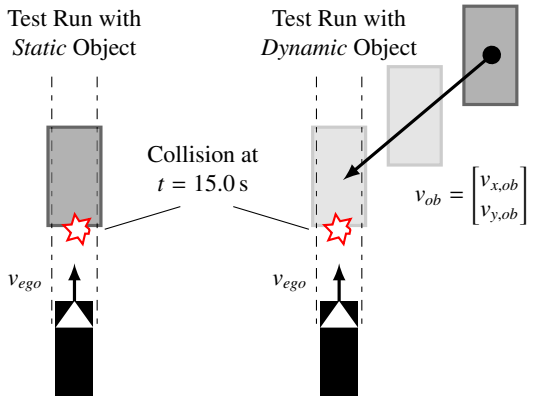

Figure 14: Generation of artificial objects in real sensor data.

Table 1: Moments of triggering for a static object.

	Time Before Potential Collision	**Collision Velocity v_c**	**Stopping Distance**
$a_{y,max} = \lvert 8\,\mathrm{m/s^2} \rvert$	0.33 s	6.90 m/s	-
$a_{y,max} = \lvert 2\,\mathrm{m/s^2} \rvert$	0.64 s	-	0.43 m
Trajectory known	0.79 s	-	1.96 m

in Figure 15(f). Here the system initiates emergency braking due to completely occupied trajectories for 5 time steps since $t = 14.25$ s in Figure 15(e).

It is important to mention that the limitation in acceleration for the operator allows a faster reaction than in conventional braking systems. Assuming a static object in the left front of the ego-vehicle, the triggering of a braking maneuver can happen earlier because of more limited vehicle dynamics. Figure 16 illustrates the different trajectories 0.34 s before a potential collision between conventional systems, teleoperation with limited acceleration range and teleoperation with one known trajectory, as presented in (Gnatzig et al., 2012).

The setting in Figure 16(a) shows still one drivable trajectory in conventional systems and therefore, no triggering of a braking maneuver occurs. The method presented with a range of accelerations for the operator of up to $\lvert 2\,\mathrm{m/s^2} \rvert$ can trigger already at $t = 14.35$ s, 0.65 s before a potential collision. Applying a trajectory-based shared autonomy control of the vehicle, the trajectory determined by the operator is known. In this case the braking system has to check only this trajectory and can trigger even earlier. All results for the moments of triggering are summarized in Table 1.

6 SYSTEM PERFORMANCE

The sensor data processing presented operates fast and effectively exclusively with sensor raw data. The main problem is caused by the measurement errors of the lidar sensor used that are not detected reliably. The particle filter is able to track and predict moving measurement points briskly and robustly.

In the situation assessment there are still faulty activations because of measurement faults as described above. But for correct sensor data the intervention concept based on provided accelerations for the operator is well suited for teleoperated driving.

The computations in MATLAB code for a time increment in real time of $dt = 0.01$ s actually needs $dt_{calc} = 0.022$ s on a consumer Intel® Core™ i7-2620M CPU @ 2.7 GHz PC running Windows 7 Professional with 8 GB RAM. But with the possibility of externalizing code in a C- or Fortran-compiler, programs can easily run 10 to 20 times faster, which makes the system presented real-time capable (Getreuer, 2009).

7 CONCLUSION

This paper has presented a method for an emergency braking system based on a lidar sensor. With sensor data processing taking place at raw data level, it has been possible to reduce the number of measurement points significantly. By grouping points and selecting two of them from the lateral edge, the object velocity has mapped very well and in this way moving objects have been tracked and predicted robustly. The situation assessment has compared these predictions with possible trajectories of the ego-vehicle and derived a decision as to whether braking is required or not.

The analysis of test runs has demonstrated the functional capability and the short response time of the system. In speed ranges of city traffic, collisions can be avoided successfully. The emergency braking system with calculations at raw data level enables a fast reaction time. Furthermore, the application of this system in teleoperated vehicles possesses two main advantages compared to conventional automatic braking systems: First, a lateral acceleration of $2\,\mathrm{m/s^2}$ will not be exceeded, which offers the possibility to react earlier. Second, the trajectory the vehicle follows can be clearly specified, which makes the decision process more precise. Simulation examples show the advantages of the teleoperated system compared to conventional systems, where collisions can be avoided successfully.

8 FURTHER RESEARCH

Since lidar sensors are influenced by environmental conditions, the choice of alternatives or sensor fusion could further improve its robustness. Combined object detection could make possible reactions which depend on more than measurement points. In this way a more detailed and adapted motion model of detected objects in the particle filter would be able to predict

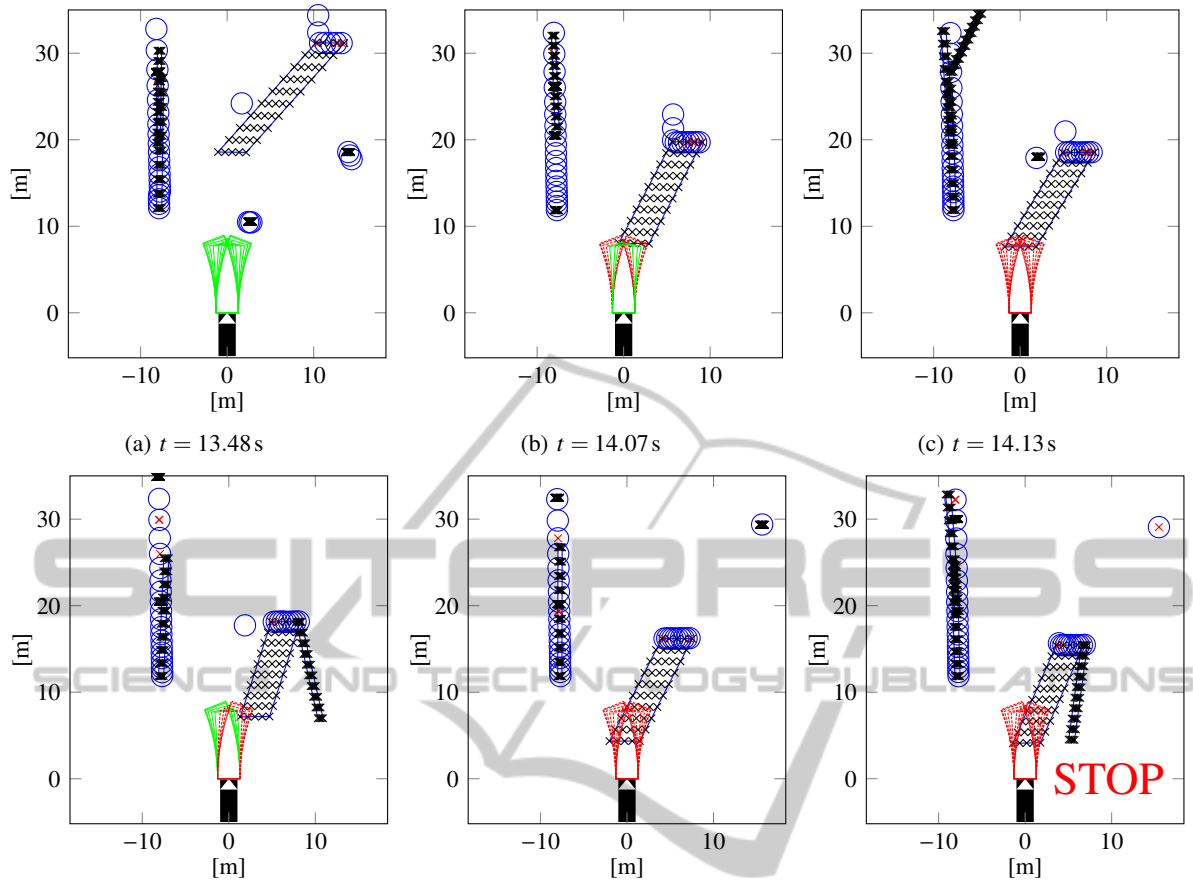

(a) $t = 13.48\,\mathrm{s}$ (b) $t = 14.07\,\mathrm{s}$ (c) $t = 14.13\,\mathrm{s}$

(d) $t = 14.15\,\mathrm{s}$ (e) $t = 14.25\,\mathrm{s}$ (f) $t = 14.29\,\mathrm{s}$

Figure 15: Triggering of an emergency braking maneuver.

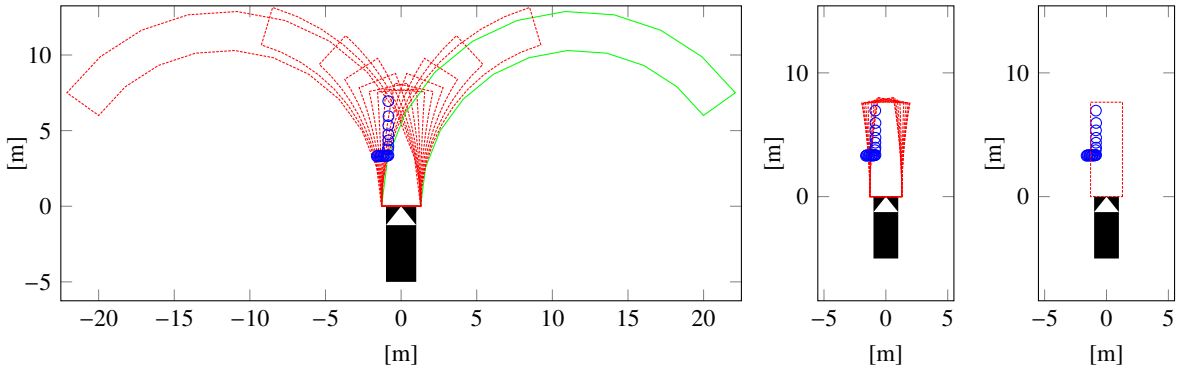

(a) Conventional system with $a_{y,max} = |8\,\mathrm{m/s^2}|$ (b) Teleoperation with $a_{y,max} = |2\,\mathrm{m/s^2}|$ (c) Teleoperation with one known trajectory

Figure 16: Trajectories 0.34 s before a potential collision in conventional driving compared to teleoperated driving ($v_{ego} = 9.5\,\mathrm{m/s}$).

movements better. Thereby a specific braking reaction can be attributed to an object. The already existing video cameras of a teleoperated vehicle can be used for that sensor data fusion. But all refinements of models and an increasing level of detail must be weighed up against a slower reaction time of the system. Even though this system has been evaluated in simulation, it still needs to be analyzed during field tests to corroborate its validity.

REFERENCES

Almeida, J. and Araujo, R. (2008). Tracking multiple moving objects in a dynamic environment for autonomous navigation. *2008 10th IEEE International Workshop on Advanced Motion Control*, pages 21–26.

Biral, F., Da Lio, M., and Bertolazzi, E. (2005). Combining safety margins and user preferences into a driving criterion for optimal control-based computation of reference maneuvers for an ADAS of the next generation. In *2005 IEEE Intelligent Vehicles Symposium proceedings*, pages 36–41, Las Vegas, Nevada, USA.

Chen, J., Haas, E. C., and Barnes, M. J. (2007). Human performance issues and user interface design for teleoperated robots. *IEEE Transactions on Systems, Man and Cybernetics, Part C (Applications and Reviews)*, 37(6):1231–1245.

Diermeyer, F., Gnatzig, S., Chucholowski, F., Tang, T., and Lienkamp, M. (2011). Der Mensch als Sensor - Der Weg zum teleoperierten Fahren. In *AAET 2011 - Automatisierungssysteme, Assistenzsysteme und eingebettete Systeme fuer Transportmittel Symposium am 09. und 10.02.2011*, pages 119–135. Inteligente Transport- und Verkehrssysteme und -dienste Niedersachsen e.V., Braunschweig.

Getreuer, P. (2009). Writing Fast MATLAB Code.

Gnatzig, S., Chucholowski, F., Tang, T., and Lienkamp, M. (2013). A System Design for Teleoperated Road Vehicles. In *ICINCO2013, 10th International Conference on Informatics in Control, Automation and Robotics*, pages 231–238, Reykjavik.

Gnatzig, S., Schuller, F., and Lienkamp, M. (2012). Human-machine interaction as key technology for driverless driving - A trajectory-based shared autonomy control approach. In *2012 IEEE RO-MAN: The 21st IEEE International Symposium on Robot and Human Interactive Communication*, pages 913–918, Paris. IEEE.

Grover, C., Knight, I., Okoro, F., Simmons, I., Couper, G., Massie, P., and Smith, B. (2013). Automated emergency brake systems: Technical requirements, costs and benefits. *TRL Limited*.

Hackenberg, U. and Heißing, B. (1982). Die fahrdynamischen Leistungen des Fahrer-Fahrzeug-Systems im Straßenverkehr. *ATZ*, 84:341–345.

Hong, D., Kang, H.-J., and Yoon, P. (2008). Control Concept for Forward Collision Warning and Mitigation. In *Proceedings of the 17th World Congress - The International Federation of Automatic Control*, pages 8532–8533, Seoul.

Jansson, J., Johansson, J., and Gustafsson, F. (2002). Decision making for collision avoidance systems. *Society of Automotive Engineers, Inc.*

Kämpchen, N. (2007). *Feature-Level Fusion of Laser Scanner and Video Data for Advanced Driver Assistance Systems*. Dissertation, Universität Ulm.

Kopischke, S. (2000). *Entwicklung einer Notbremsfunktion mit Rapid- Prototyping- Methoden*. Dissertation, Technische Universität Carolo-Wilhelmina zu Braunschweig.

Ristic, B., Arulampalam, S., and Gordon, N. (2004). *Beyond the Kalman Filter: Particle Filters for Tracking Applications*. Artech House.

Schmidt, C., Oechsle, F., and Branz, W. (2005). Untersuchungen zu letztmöglichen Ausweichmanövern für stehende und bewegte Hindernisse. In *3. FAS-Workshop*, Walting.

Stämpfle, M. and Branz, W. (2008). Kollisionsvermeidung im Längsverkehr - die Vision vom unfallfreien Fahren rückt näher. In *3. Tagung Aktive Sicherheit durch Fahrerassistenz*, München.

Tang, T., Kurkowski, J., and Lienkamp, M. (2013). Teleoperated Road Vehicles : A Novel Study on the Effect of Blur on Speed Perception. *International Journal of Advanced Robotic Systems*, 10.

Thrun, S. (2013). Car localization with particle filter. In *Lecture: Artificial Intelligence for Robotics*, chapter 3.

Thuy, M. and Puente Leon, F. (2009). Non-linear, shape independent object tracking based on 2D lidar data. *2009 IEEE Intelligent Vehicles Symposium*, pages 532–537.

Ware, J. and Pan, Y.-J. (2011). Realisation of a bilaterally teleoperated robotic vehicle platform with passivity control. *IET Control Theory & Applications*, 5(8):952–962.

Wegscheider, M. and Prokop, G. (2005). Modellbasierte Komfortbewertung von Fahrerassistenzsystemen. *VDI Berichte*, 1900:17–36.